Journal of Applied Mathematics and Computing
https://doi.org/10.1007/s12190-020-01325-8

ORIGINAL RESEARCH

Mathematical model of the immune response to dengue virus

Miller Cerón Gómez[1] · **Hyun Mo Yang**[2]

Received: 3 September 2019
© Korean Society for Informatics and Computational Applied Mathematics 2020

Abstract
Dengue disease is caused by an infected mosquito bite and manifests in different clinical symptoms. The complexity of the pathogenesis of dengue virus and the limitations of biological knowledge have been barriers to completely understanding the progress of this disease. To address this concern, we developed a mathematical model of the immune response to eliminate dengue virus. The model considered both cellular and humoral immune responses, and we evaluated their contributions to the clearance of dengue virus.We also performed global sensitivity analysis and parameters estimation using clinical data. We found the global stability for virus-free equilibrium and for the virus-presence equilibrium, we concluded that to avoid oscillations in the model and to control the viral load, a strong proliferation of cytotoxic cells must prevail. However, if there exists a weak proliferation of cytotoxic cells, the way to avoid instabilities is to either inhibit the differentiation of T-CD4+ helper cells in Th1 cells or increase the proliferation of B cells.

Keywords Dengue virus · Adaptive immune response · Humoral and cellular immune responses · Deterministic model · Net reproduction number of virus

Mathematics Subject Classification 92B05 · 92C50

1 Introduction

Dengue virus (DENV), a flavivirus of a large family of related positive-strand RNA viruses (*Flaviviridae*), is transmitted by arthropod of the genus *Aedes* and is prevalent in different parts of the world, actually there are four DENV serotypes (DENV-1,

✉ Miller Cerón Gómez
millercg@udenar.edu.co

1 Universidad de Nariño, Torobajo, Calle 18 Carrera 50, Pasto, Colombia

2 Universidade Estadual de Campinas, Cidade Universitária "Zeferino Vaz", Campinas CEP 13083-970, Brazil

Published online: 18 February 2020

DENV-2, DENV-3, and DENV-4). As a result of being pathogenic for humans and capable of transmission in heavily populated areas, dengue virus (arbovirus) can cause widespread and serious epidemics, which constitute one of the major public health problems in many tropical and subtropical regions of the world where *Aedes aegypti* and other appropriate mosquito vectors are present.

After an infectious mosquito bite, DENV attaches to the surface of host cells through an interaction of E-protein (type I membrane protein) with one or more receptors, and several cell surface proteins have been described as a candidate for flavivirus receptors. After binding, virions are taken up by receptor-mediated endocytosis, although direct fusion at the plasma membrane has also been observed. Virions are found in uncoated prelysosomal vesicles, where an acid-catalyzed membrane fusion is thought to release the nucleocapsid into the cytoplasm. Following entry and fusion, nucleocapsids are presumably disassembled, genomic RNA is translated and replication of RNA is initiated. Nascent virions are transported by bulk flow through the secretory pathway to the cell surface, where exocytosis occurs [15]. Dengue virus replicates in local lymph nodes and within 2–3 days disseminates via the blood to various tissues. Virus circulates in the blood typically for 5 days in infected monocytes/macrophages, and to a lesser degree in B cells and T cells. It also replicates in the skin and reactive spleen lymphoid cells. However, the quick replication of the virus is contained by the immune response. The rise of levels of serum neutralizing antibodies is correlated with the clearance of viremia, but immunity is associated with both humoral and cellular immune responses [19].

There are many mathematical models describing the transmission and spreading of dengue infection in human population [9,13,14,32,34–36]. Those models are allowed to evaluate some aspects of dengue epidemics, such as the populational risk of dengue infection and control (measured by basic reproduction number, denoted by R_0), the dependence of dengue incidence with seasonally varying temperature and rain, and the transovarial transmission. Besides this macroscopic approach, mathematical models can deal with the interaction of dengue virus with immune response mounted by humans. Indeed, there are mathematical models of DENV that describe the interaction between DENV and the target cells, or the interaction among DENV, the target cells and the immune system [2,3,6,11,24,25,27,29]. However, those models did not deal with humoral and cellular immune response to dengue virus, except the paper [27]; our mathematical model instead try to describe the adaptive immune response activated by the T helper cells, assuming that the innate immune system failed to contain the virus injected by infected mosquitoes. In the modelling, besides taking into account DENV and target cells, our model considers T-CD4+ helper cells differentiating into Th1 cells or Th2 cells.

We stress the fact that a primary dengue infection is being considered here, and the antibody dependent enhancement due to secondary dengue infection is not dealt with, see [4] to view this consideration.

The paper is structured as follows. In Sect. 2, a model for primary dengue infection interacting with an adaptive immune response is presented. Section 3 presents the analysis of the model (equilibrium points and the stability analysis)

Table 1 Definition of the variables of the model given by Eqs. (1)–(4)

Symbol	Definition
S	Target cells
I	Infected cells
V	Dengue virus
T_0	Naive Th0 helper cells
T_1	Th1 helper cells
T_2	Th2 helper cells
T_{cr}	Naive cytotoxic T-CD8+ cells
T_{ca}	Activated cytotoxic T-CD8+ cells
B_r	Resting B cells
B_a	Activated B cells

Section 4 presents the numerical simulation to evaluate the immune response. Section 5 presents the estimation and sensitivity of the model parameters. Discussion is given in Sect. 6.

2 Model formulation

Dengue virus circulates due to the interaction between human and mosquito populations in urban areas. A primary infection by one serotype of dengue virus is being considered in the modelling. A model dealing with a second serotype of DENV becomes complex. For instance, antibody dependent enhancement due to secondary dengue infection may occur in the first days just after the virus inoculation concomitantly with the immune system mounting a response to this secondary infection.

We model a primary infection by DENV and the reaction of adaptive immune response as described in the introduction. To do this, we use cells involved in the infection and the immune response to dengue virus. The model variables are: S—target cells, I—infected cells, V—dengue virus; T-CD4+ helper cells Th0, Th1 and Th2 denoted by T_0, T_1 and T_2; B_r—naive B cells, B_a—B plasma cells; T_{cr}—T-CD8+ naive cells; T_{ca}—T-CD8+ activated cells. The role of each of these variables is described below. In Table 1 a summary of variables of the model is presented.

Firstly, let us describe the dynamics of DENV and adaptive immune response without interaction. We are assuming that innate immune response did not contain DENV. All model parameters are constant and per-capita rates, unless explicitly cited. DENV infects a pool of target cells, such as skin cells, dendritic cells, and monocytes/macrophages. We assume that this pool of cells (S) is regulated by homeostasis, that is, they are produced (in different sites) at a total rate k_s, and die at a rate μ_s. These cells are infected by DENV at a rate β_I, and become infected cells (I) which have, besides the natural mortality rate μ_s, an additional death rate μ_I due to apoptosis. We assume that on average N_2 viruses can infected each

cell. For simplicity, we assume that nascent virus are released in the tissues as soon as infected cells die ($\mu_s + \mu_I$), and each dying cell releases on average N_1 virions. On the other hand, the number of DENV in humans (V) decreases at a constant mortality rate μ_v. The dynamics of DENV without immune response is given by

$$\begin{cases} \frac{dS}{dt} = k_s - \beta_I SV - \mu_s S \\ \frac{dI}{dt} = \beta_I SV - (\mu_s + \mu_I)I \\ \frac{dV}{dt} = N_1(\mu_s + \mu_I)I - N_2\beta_I SV - \mu_v V. \end{cases}$$

As we have done with target cells, we assume that lymphocytes maintain their size by homeostasis. The naive T-CD4+ helper cells (T_0) are produced in the thymus at total rate k_0 and die at rate μ_0. The naive T-CD8+ cytotoxic cells (T_{cr}) are produced also in the thymus at total rate k_{cr} and die at rate μ_{cr}. The naive B cells (B_r) are produced in the bone marrow at total rate k_r and die at rate μ_r. Hence, the resting populations of lymphocyte cells obey

$$\begin{cases} \frac{dT_0}{dt} = k_0 - \mu_0 T_0 \\ \frac{dT_{cr}}{dt} = k_{cr} - \mu_{cr} T_{cr} \\ \frac{dB_r}{dt} = k_r - \mu_r B_r. \end{cases}$$

Now, we describe the adaptive immune system responding to face the invading DENV. We assume that both humoral and cellular immune responses are acting to eliminate the virus, and, for simplicity, we are not taking into account the inhibition of humoral response in the cellular response (one of the Th2 cytokines, IL-10, acts to decrease the rate of proliferation of Th1 cells), and vice-versa (IFN-γ produced by Th1 cells decreases the rate of proliferation of Th2 cells).

After the innate immune response is left behind, the infected cells travel to lymph node to activate the adaptive immune response. The different signals emitted by the infected cells and the innate immune response will differentiate Th0 cells into Th1 and Th2 helper cells, in order to activate balanced humoral and cellular immune responses to fade out the dengue infection. The naive Th0 helper cells (T_0) are capable of differentiating into Th1 cells (T_1) by the signalization of cytokine IL-12 and into Th2 cells (T_2) by the cytokine IL-4. Instead of cytokines, we assume that these differentiations are mediated by the presence and the stimulus of infected cells (I) and virus (V), at rates $\gamma_1 I$ and $\gamma_2 V$, respectively. The death rates of these activated Th1 and Th2 helper cells are μ_1 and μ_2.

The humoral pathway response is triggered when Th2 helper cells (T_2) activate resting B cells (B_r) into activated B cells (B_a) at a rate $\alpha_r T_2$. The plasma cells (B_a) proliferate at rate $\alpha_a V$ and decay at rate μ_a, and these cells secrete antibodies with improved affinity to DENV. The formation of antigen-antibody complex is proportional to B_a, and the phagocytosis of this complex occurs at rate $\alpha_v B_a$.

In a similar way, the naive T-CD8+ cells (T_{cr}) are activated by Th1 helper cells (T_1) at rate $\alpha_{cr} T_1$. The activated T-CD8+ cells (T_{ca}) proliferate at rate $\alpha_{ca} I$ and decay at

rate μ_{ca}, and these cells, receiving the correct signal, will perform the lysis of infected cells at rate $\alpha_I T_{ca}$.

Based on above assumptions and description with respect to the interaction between DENV and immune response, the dynamics of this interaction is given by

$$\begin{cases} \frac{dS}{dt} = k_s - \beta_I V S - \mu_s S \\ \frac{dI}{dt} = \beta_I V S - \alpha_I T_{ca} I - (\mu_s + \mu_I) I \\ \frac{dV}{dt} = N_1(\mu_s + \mu_I) I - N_2 \beta_I S V - \alpha_v B_a V - \mu_v V, \end{cases} \tag{1}$$

which describes the vital dynamics of virus, and the action of humoral and immune responses to eliminate it, and the Eq. (2) describes the differentiation of Th0 cells into Th1 and Th2 cells,

$$\frac{dT_0}{dt} = k_0 - \gamma_1 I T_0 - \gamma_2 V T_0 - \mu_0 T_0, \tag{2}$$

Finally the system of equations (3) and (4), describe the cellular pathway of immune response to clearance DENV, and the humoral pathway of immune response, respectively.

$$\begin{cases} \frac{dT_1}{dt} = \gamma_1 I T_0 - \mu_1 T_1 \\ \frac{dT_{cr}}{dt} = k_{cr} - \alpha_{cr} T_1 T_{cr} - \mu_{cr} T_{cr} \\ \frac{dT_{ca}}{dt} = \alpha_{cr} T_1 T_{cr} + \alpha_{ca} I T_{ca} - \mu_{ca} T_{ca}, \end{cases} \tag{3}$$

$$\begin{cases} \frac{dT_2}{dt} = \gamma_2 V T_0 - \mu_2 T_2 \\ \frac{dB_r}{dt} = k_r - \alpha_r T_2 B_r - \mu_r B_r \\ \frac{dB_a}{dt} = \alpha_r T_2 B_r + \alpha_a V B_a - \mu_a B_a, \end{cases} \tag{4}$$

The system of equations (1)–(4) describes the invasion of virus that evaded innate immune response, that initiates unconstrained increasing of the viremia. However, after the mounting of the adaptive immune response, the virus is contained, or even eliminated. The model does not take into account the apoptosis of the activated lymphocytes after the containment of the virus. The apoptosis can be introduced in the model allowing the parameters γ_1, γ_2, μ_{ca} and μ_a be dependent on variables I and V. For instance, the mortality rates μ_{ca} and μ_a can be written as

$$\mu_{ca} = \begin{cases} \mu_{ca}, \text{ if } I > I^* \\ \infty, \text{ if } I \leq I^* \end{cases} \text{ and } \mu_a = \begin{cases} \mu_a, \text{ if } V > V^* \\ \infty, \text{ if } V \leq V^* \end{cases},$$

where I^* and V^* are very small numbers such that infected cells and virus could be considered eliminated, a model considering this approximation can be found in [33].

3 Mathematical Analysis

3.1 Positively invariant set

$$\mathcal{A} = \left\{ P \in \mathbb{R}^{10}_{+0} : N_1 S + NI + V + T_0 + T_1 + T_2 + \frac{\alpha_v}{\alpha_a}(B_r + B_a) + \theta(T_{cr} + T_{ca}) \leq \frac{\bar{k}}{\delta}, I < \frac{\mu_{ca}}{\alpha_{ca}}, V < \frac{\mu_a}{\alpha_a} \right\}, \tag{5}$$

where $P = (S, I, V, T_0, T_1, T_2, B_r, B_a, T_{cr}, T_{ca})$, $N = (N_1 + N_2)$, $\theta = \frac{N\alpha_I}{\alpha_{ca}}$, $\bar{k} = k_0 + N_1 k_s + \frac{\alpha_v}{\alpha_a} k_r + \theta k_{cr}$ and $\delta = \min\left\{ \mu_s, \mu_v, \mu_0, \mu_1, \mu_2, \mu_r, \mu_a, \mu_{cr}, \mu_{ca}, \frac{N_2(\mu_s + \mu_I)}{N} \right\}$.

Lemma 1 *The set $\mathcal{A}$ is positively invariant with respect to system (1)–(4).*

Proof let $P_0 \in \mathcal{A}$ be the initial condition of the system (1)–(4) and

$$\Phi = N_1 S + NI + V + T_0 + T_1 + T_2 + \frac{\alpha_v}{\alpha_a}(B_r + B_a) + \theta(T_{cr} + T_{ca}). \tag{6}$$

Taking the derivative of Φ with respect to t, we have:

$$\frac{d\Phi}{dt} = N_1 \frac{dS}{dt} + N\frac{dI}{dt} + \frac{dV}{dt} + \frac{dT_0}{dt} + \frac{dT_1}{dt} + \frac{dT_2}{dt} + \frac{\alpha_v}{\alpha_a}\left(\frac{dB_r}{dt} + \frac{dB_a}{dt}\right) + \theta\left(\frac{dT_{cr}}{dt} + \frac{dT_{ca}}{dt}\right)$$

replacing the equations of the system (1)–(4), we have

$$\frac{d\Phi}{dt} = N_1 k_s - N_1 \mu_s S - N_2(\mu_s + \mu_I) I - \mu_v V + k_0 - \mu_0 T_0 - \mu_1 T_1 - \mu_2 T_2 + \frac{\alpha_v}{\alpha_a}[k_r - (\mu_r B_r + \mu_a B_a)] + \theta[k_{cr} - (\mu_{cr} T_{cr} + \mu_{ca} T_{ca})],$$

which can be written as

$$\frac{d\Phi}{dt} + N_1 \mu_s S + N_2(\mu_s + \mu_I) I + \mu_v V + \mu_0 T_0 + \mu_1 T_1 + \mu_2 T_2 + \frac{\alpha_v}{\alpha_a}(\mu_r B_r + \mu_a B_a) + \theta(\mu_{cr} T_{cr} + \mu_{ca} T_{ca}) = \bar{k},$$

where $\bar{k} = k_0 + N_1 k_s + \frac{\alpha_v}{\alpha_a} k_r + \theta k_{cr}$.

If we choose $\delta = \min\left\{\mu_s, \mu_v, \mu_0, \mu_1, \mu_2, \mu_r, \mu_a, \mu_{cr}, \mu_{ca}, \frac{N_2(\mu_s+\mu_I)}{N}\right\}$, we conclude that,

$$\frac{d\Phi}{dt} + \delta\Phi \leq \bar{k}, \text{ then } \Phi \leq \frac{\bar{k}}{\delta} + \left(\Phi(0) - \frac{\bar{k}}{\delta}\right)e^{-\delta t}, \text{ for all } t \geq 0,$$

wich implies $\Phi \leq \frac{\bar{k}}{\delta}$.

3.2 Basic reproduction number

The net reproduction number of virus R_0 is given by

$$R_0 = \frac{\beta_I k_s}{\mu_v \mu_s} N_1 - \frac{\beta_I k_s}{\mu_v \mu_s} N_2 = \frac{\beta_I (N_1 - N_2) k_s}{\mu_v \mu_s}. \tag{7}$$

The term net reproduction number of virus was borrowed from epidemiology [17].

Let us interpret the threshold R_0. There are k_s/μ_s number of target cells that can be infected in a completely susceptible pool of cells. In the absence of the immune response, the average period of survival time of virus is $1/\mu_v$, and during this time a virus can infect a susceptible cell. Then, a virus, during the time period $1/\mu_v$, encounters k_s/μ_s target cells, and infects one of them with rate β_I. Hence, $\left(\beta_I k_s/\mu_s\right)/\mu_v$ is the capacity of one virus infecting one cell in a completely susceptible pool of target cells. However, there are two characteristics when dealing with infection (or penetration) of virus in a cell. First, instead of only one virus, it is considered infection by on average N_2 virions. On the other hand, instead of only one nascent virus, the infected cell releases on average N_1 virions. Hence, the first term in Eq. (7) is the average number of virions released by one infected cell, while the second term is the average number of virions penetrating one susceptible cell. Therefore, R_0 is the net reproduction of nascent virions originated from N_2 virions penetrating in a single cell. Biologically, the minimum number of virions infecting one cell is 1, and the net reproduction number must be positive (if negative, P_0 is always stable), hence we must have $1 \leq N_2 < N_1$.

The system of equations (1)–(4) has two equilibrium points. The first equilibrium point represents a clearance of infection by the effective action of immune response, which we call the virus-free equilibrium point P_0, which is given by

$$P_0 = \left(\frac{k_s}{\mu_s}, 0, 0, \frac{k_0}{\mu_0}, 0, 0, \frac{k_r}{\mu_r}, 0, \frac{k_{cr}}{\mu_{cr}}, 0\right).$$

The other equilibrium point P_1 represents a persistent infection by DENV, which is given by

$$P_1 = (S^*, I^*, V^*, T_0^*, T_1^*, T_2^*, B_r^*, B_a^*, T_{cr}^*, T_{ca}^*),$$

where the coordinates are given in Sect. 3.4. Numerically, it was shown that there is a unique biologically feasible steady state P_1 (all coordinates are non-negatives).

3.3 Stability of virus-free equilibrium

Let P_0 be the virus-free equilibrium point which is obtained when we assume that non particle of dengue virus is in the body, i.e., $V = 0$, then

$$P_0 = \left(\frac{k_s}{\mu_s}, 0, 0, \frac{k_0}{\mu_0}, 0, 0, \frac{k_r}{\mu_r}, 0, \frac{k_{cr}}{\mu_{cr}}, 0\right).$$

For this point, the local and global stability is analyzed, and the threshold R_0 is obtained.

Theorem 1 *The virus-free equilibrium P_0 is locally asymptotically stable if $R_0 < 1$ and is unstable if $R_0 > 1$.*

Proof To prove the local stability at point P_0, we show that the eigenvalues of the Jacobian matrix of the system (1)–(4) at P_0 are negative or have a negative real part . The characteristic polynomial evaluated at point P_0 is $p(\lambda) = |A - \lambda I_{3\times 3}||B - \lambda I_{7\times 7}|$, where

$$A = \begin{pmatrix} -\mu_s & 0 & -\frac{\beta_I k_s}{\mu_s} \\ 0 & -\mu_s - \mu_I & \frac{\beta_I k_s}{\mu_s} \\ 0 & (\mu_s + \mu_I) N_1 & -\frac{\beta_I k_s N_2}{\mu_s} - \mu_v \end{pmatrix},$$

$$B = \begin{pmatrix} -\mu_0 & 0 & 0 & 0 & 0 & 0 & 0 \\ 0 & -\mu_1 & 0 & 0 & 0 & 0 & 0 \\ 0 & 0 & -\mu_2 & 0 & 0 & 0 & 0 \\ 0 & 0 & -\frac{\alpha_r k_r}{\mu_r} & -\mu_r & 0 & 0 & 0 \\ 0 & 0 & \frac{\alpha_r k_r}{\mu_r} & 0 & -\mu_a & 0 & 0 \\ 0 & -\frac{\alpha_{cr} k_{cr}}{\mu_{cr}} & 0 & 0 & 0 & -\mu_{cr} & 0 \\ 0 & \frac{\alpha_{cr} k_{cr}}{\mu_{cr}} & 0 & 0 & 0 & 0 & -\mu_{ca} \end{pmatrix}.$$

The roots of polynomial $p(\lambda)$ are given by $-\mu_s, -\mu_0, -\mu_1, -\mu_2, -\mu_r, -\mu_a, -\mu_{cr}$, $-\mu_{ca}$ plus the solutions of following second degree polynomial:

$$\lambda^2 + \left(\mu_s + \mu_I + \mu_v + \frac{\beta_I k_s N_2}{\mu_s}\right)\lambda + (\mu_s + \mu_I)\mu_v (1 - R_0),$$

where $R_0 = \dfrac{\beta_I (N_1 - N_2) k_s}{\mu_v \mu_s}$. Then by the Routh Hurwitz criteria [10] (pg 230), the virus-free equilibrium P_0 is locally asymptotically stable if the coefficients of second degree polynomial are positive, i.e., if $R_0 < 1$, and it is unstable if $R_0 > 1$.

Remark 1 When $R_0 = 1$ we have a zero eigenvalue and all others have negative real part, that is, the point P_0 is non hyperbolic. We shall prove that this point is globally asymptotically stable if $R_0 < 1$.

3.3.1 Global stability of disease-free equilibrium

Theorem 2 *The point P_0 is globally asymptotically stable if $R_0 < 1$ in $\mathcal{A}$.*

Proof To proof this, we start to show that the system (1) is globally asymptotically stable if $R_0 < 1$ when T_{ca} and B_a are bounded non-negative functions. Finally we use this result to proof that the point $\left(\frac{k_0}{\mu_0}, 0, 0, \frac{k_r}{\mu_r}, 0, \frac{k_{cr}}{\mu_{cr}}, 0\right)$ is globally asymptotically stable for the system (2)–(4).

Firstly, observe that T_{ca} and B_a are bounded by Lemma 1. Let L be the function defined as follows $L : \Omega \to \mathbb{R}$, where

$$\Omega = \{(S, I, V) : S > 0, I \geq 0, V \geq 0\}$$

and

$$L = (N_1 - N_2)\left(S - \frac{k_s}{\mu_s} - \frac{k_s}{\mu_s}\ln\frac{\mu_s S}{k_s}\right) + N_1 I + V.$$

It is easily to check that $L(\frac{k_s}{\mu_s}, 0, 0) = 0$ and $L > 0$ for all point different of $(\frac{k_s}{\mu_s}, 0, 0)$. Besides, the orbital derivative of L along solutions of the system (1) is given by

$$\dot{L}=(N_1-N_2)\left(1-\frac{k_s}{\mu_s S}\right)\left(k_s-\beta_I SV-\mu_s S\right)+N_1\left[\beta_I SV - \alpha_I T_{ca} I - (\mu_s + \mu_I)I\right] + \left[N_1(\mu_s + \mu_I)I - N_2\beta_I SV - \alpha_v B_a V - \mu_v V\right],$$

which is equivalent to

$$\dot{L} = -(N_1 - N_2)\mu_s S\left(1 - \frac{k_s}{\mu_s S}\right)^2 + (R_0 - 1)\mu_v V - N_1\alpha_I T_{ca} I - \alpha_v B_a V.$$

From last equation $\dot{L} < 0$ in $\Omega - \{(\frac{k_s}{\mu_s}, 0, 0)\}$, if and only if $R_0 < 1$. Then the point $(\frac{k_s}{\mu_s}, 0, 0)$ is global asymptotically stable for the system (1). It means that $(S, I, V) \to (\frac{k_s}{\mu_s}, 0, 0)$ as $t \to \infty$ and $R_0 < 1$, which implies that the system (2)–(4) could be analyze as follow:

In the Eq. (2), we can see that

$$\frac{dT_0}{dt} = k_0 - \gamma_1 I T_0 - \gamma_2 V T_0 - \mu_0 T_0 \Longrightarrow \frac{dT_0}{dt} = k_0 - \mu_0 T_0, \quad \text{then } T_0 \to \frac{k_0}{\mu_0}$$

and in the system of equations (3), we have

$$\frac{dT_1}{dt} = \gamma_1 I T_0 - \mu_1 T_1 \implies \frac{dT_1}{dt} = -\mu_1 T_1, \text{ then } T_1 \to 0 \text{ which implies that}$$

$$\frac{dT_{cr}}{dt} = k_{cr} - \alpha_{cr} T_1 T_{cr} - \mu_{cr} T_{cr} \implies \frac{dT_{cr}}{dt} = k_{cr} - \mu_{cr} T_{cr}, \text{ then } T_{cr} \to \frac{k_{cr}}{\mu_{cr}}$$
$$\frac{dT_{ca}}{dt} = \alpha_{cr} T_1 T_{cr} + \alpha_{ca} I T_{ca} - \mu_{ca} T_{ca} \implies \frac{dT_{ca}}{dt} = -\mu_{ca} T_{ca}, \text{ then } T_{ca} \to 0.$$

Similarly, we can see that in the system of equations (4), we can have $T_2 \to 0$, $B_r \to \frac{k_r}{\mu_r}$ and $B_a \to 0$, when $(S, I, V) \to (\frac{k_s}{\mu_s}, 0, 0)$ as $t \to \infty$ and $R_0 < 1$.

3.4 Virus presence equilibrium

Theorem 1 implies that the net reproduction number R_0 is a parameter of bifurcation. When $R_0 > 1$, the system has two equilibria, but just one of this solution is biologically feasible (V has a positive value).

Let $P_1 = (S^*, I^*, V^*, T_0^*, T_1^*, T_2^*, B_r^*, B_a^*, T_{cr}^*, T_{ca}^*)$ be the non-trivial equilibrium point. The coordinates of P_1 are given by:

$$\begin{aligned}
S^* &= \frac{k_s}{\beta_I V^* + \mu_s} \\
I^* &= \frac{\phi(V^*)V^*}{N_1(\mu_I + \mu_s)} \\
T_0^* &= \frac{k_0 N_1(\mu_I + \mu_s)}{\psi(V^*)} \\
T_1^* &= \frac{\gamma_1 k_0 \phi(V^*)V^*}{\mu_1 \psi(V^*)} \\
T_2^* &= \frac{\gamma_2 k_0 N_1(\mu_I + \mu_s)V^*}{\mu_2 \psi(V^*)} \\
B_r^* &= \frac{k_r \mu_2 \psi(V^*)}{\alpha_r \gamma_2 k_0 N_1(\mu_I + \mu_s)V^* + \mu_r \mu_2 \psi(V^*)} \\
B_a^* &= \frac{-\varphi(V^*) + \sqrt{\varphi(V^*)^2 + 4(\mu_a - \alpha_a V^*)\xi\eta V^{*2}}}{2(\mu_a - \alpha_a V^*)\xi V^*} \\
T_{cr}^* &= \frac{k_{cr}\mu_1 \psi(V^*)}{\theta\phi(V^*)V^* + \mu_{cr}\mu_1 \bar{\sigma}(V^*)} \\
T_{ca}^* &= \frac{\alpha_{cr} k_{cr} \gamma_1 k_0 \phi(V^*)V^*}{(\mu_{ca} - \alpha_{ca} I^*)\{\theta\phi(V^*)V^* + \mu_{cr}\mu_1 \bar{\sigma}(V^*)\}},
\end{aligned} \tag{8}$$

where

$$\begin{aligned}
\xi &= \mu_r \mu_2 \gamma_1 \alpha_v \\
\eta &= \alpha_r k_r \gamma_2 k_0 N_1(\mu_I + \mu_s) \\
\theta &= (\alpha_{cr}\gamma_1 k_0 + \mu_{cr}\mu_1\gamma_1) \\
\varphi(V^*) &= (\mu_a - \alpha_a V^*)\left\{\frac{\eta}{k_r}V^* + \mu_r\mu_2[\gamma_1(N_2\beta_I S^* + \mu_v)V^* + (\gamma_2 V^* + \mu_0)N_1(\mu_I + \mu_s)]\right\}
\end{aligned}$$

$$\phi(V^*) = \frac{\alpha_v\left(-\varphi(V^*) + \sqrt{\varphi(V^*)^2 + 4(\mu_a - \alpha_a V^*)\xi\eta V^{*2}}\right)}{2(\mu_a - \alpha_a V^*)\xi V^*} + \frac{N_2\beta_I k_s}{(\beta_I V^* + \mu_s)} + \mu_v$$
$$\psi(V^*) = \gamma_1\phi(V^*)V^* + (\gamma_2 V^* + \mu_0)N_1(\mu_I + \mu_s)$$
$$\bar{\sigma}(V^*) = (\gamma_2 V^* + \mu_0)N_1(\mu_I + \mu_s),$$

and V^* is positive solution of the equation

$$\chi(V) = \chi_1(V)\chi_2(V)\chi_3(V) - g(V) = 0, \tag{9}$$

and

$$\chi_1(V) = [((N_1 - N_2)\beta_I k_s - \mu_v(\beta_I V + \mu_s))2(\mu_a - \alpha_a V)\xi V - \alpha_v\bar{B}_a(\beta_I V + \mu_s)]$$
$$\chi_2(V) = [(\mu_{ca}N_1(\mu_I + \mu_s) - \alpha_{ca}\mu_v V)(\beta_I V + \mu_s) - \alpha_{ca}N_2\beta_I k_s V]2(\mu_a - \alpha_a V)\xi - \alpha_{ca}\alpha_v\bar{B}_a(\beta_I V + \mu_s)$$
$$\chi_3(V) = \{[\theta(N_2\beta_I k_s + \mu_v(\beta_I V + \mu_s))V + \mu_{cr}\mu_1\bar{\sigma}(\beta_I V + \mu_s)]2(\mu_a - \alpha_a V)\xi + \theta\alpha_v\bar{B}_a(\beta_I V + \mu_s)\}$$
$$g(V) = \xi b\left[(N_2\beta_I k_s + \mu_v(\beta_I V + \mu_s))2(\mu_a - \alpha_a V)\xi V + \alpha_v\bar{B}_a(\beta_I V + \mu_s)\right]^2 2(\mu_a - \alpha_a V)(\beta_I V + \mu_s)$$
$$\bar{B}_a = 2(\mu_a - \alpha_a V)\xi V B_a$$
$$b = N_1\alpha_I\alpha_{cr}k_{cr}\gamma_1 k_0.$$

Equation (9) has two positive solutions for V, but just one is feasible (positive values) if we impose the restrictions $V^* < \frac{\mu_a}{\alpha_a}$ and $I^* < \frac{\mu_{ca}}{\alpha_{ca}}$, which are necessary to get positive values of B_a^* and T_{ca}^* respectively. Figure 1 show the graphs of the function defined in (9) for the cases $\alpha_{ca} < \alpha_a$ (Fig. 1a), $\alpha_{ca} = \alpha_a$ (Fig. 1b) and $\alpha_{ca} > \alpha_a$ (Fig. 1c). In all these cases, there exists only one feasible solution.

Now we focus our attention in this point (P_1) to evaluate the humoral and cellular immune responses and present this analysis in the next section.

4 Evaluating the immune response by the differentiation of T helper cells

The immune system is very complex and every disease generates a different immune response, which arise challenges for the researchers. However, there is a well known differentiation pathway of naive Th cells into Th1 and Th2 cells mediated by chemical signaling: Th1 cells are inhibited by the cytokines IL-4 and IL-10 produced by Th2 cells, which, in turn, can be inhibited by IFN-γ produced by Th1 cells. In the model the action of these cytokines was not considered explicitly, however we can assess the inhibitory actions indirectly by parameters γ_1 and γ_2.

In this sense, we analyze the joint action of humoral and cellular immune responses for the virus-presence equilibrium, P_1, by studying the model, given by Eqs. (1)–

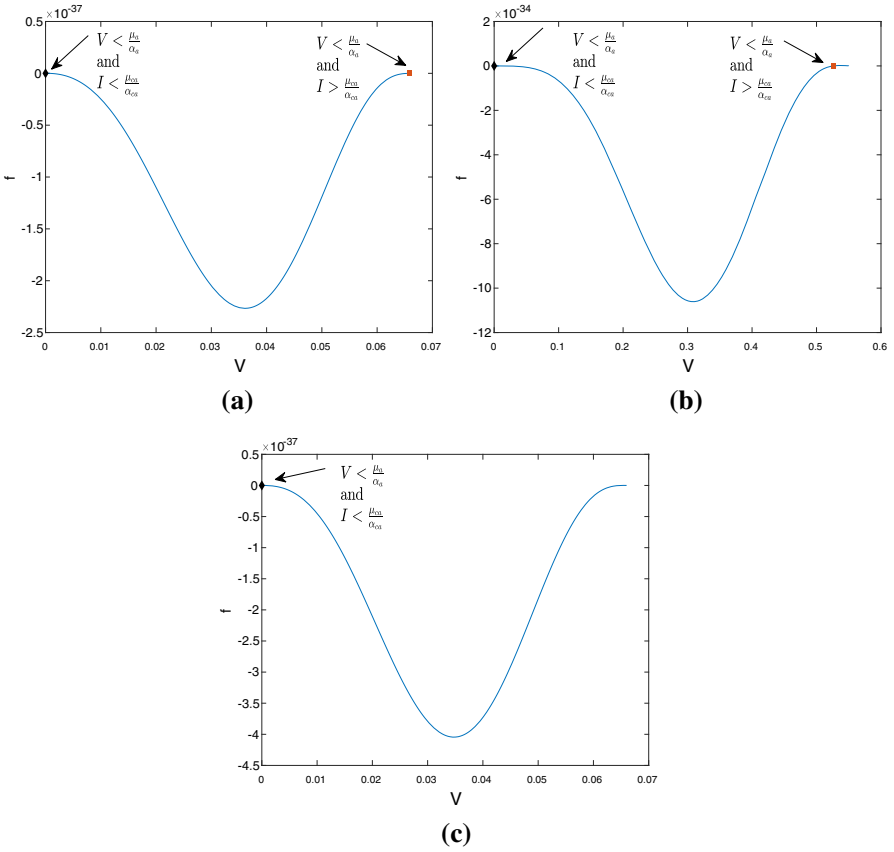

Fig. 1 The figure shows the existence of unique feasible V value. **a** Graph of the function defined in the equation (9) when $\alpha_{ca} < \alpha_a$. In this case, there exist two points satisfying $V < \frac{\mu_a}{\alpha_a}$, but just one of these points meets the inequality $I < \frac{\mu_{ca}}{\alpha_{ca}}$. The feasible point is $V = 1.774 \times 10^{-20}$, $I = 2.4303 \times^{-19}$, while the thresholds are $\frac{\mu_a}{\alpha_a} = 0.066$ and $\frac{\mu_{ca}}{\alpha_{ca}} = 0.55$. **b** Case when $\alpha_{ca} = \alpha_a$. There exists just one point that satisfies the constraints, $V < \frac{\mu_a}{\alpha_a}$ and $I < \frac{\mu_{ca}}{\alpha_{ca}}$. The values of the point are $V = 1.3906 \times 10^{-20} < \frac{\mu_a}{\alpha_a} = 0.55$ and $I = 1.9052 \times 10^{-19} < \frac{\mu_{ca}}{\alpha_{ca}} = 0.55$ **c** Finally $\alpha_{ca} > \alpha_a$. In this situation, there exists just one possible point satisfying $V < \frac{\mu_a}{\alpha_a}$ and $I < \frac{\mu_{ca}}{\alpha_{ca}}$. The point is $V = 1.606 \times 10^{-19}$ and $I = 2.2002 \times 10^{-18}$, while the thresholds are $\frac{\mu_a}{\alpha_a} = 0.066$ and $\frac{\mu_{ca}}{\alpha_{ca}} = 0.0413$

(4). In particular, we discuss how the variation of the Th helper cells differentiation parameters γ_1, γ_2 and the proliferation parameters of activated B_a and T_{ca} cells, α_a, α_{ca} respectively, affects on the dynamic of the general model.

In order to do this, we use the values of the parameters given in Table 2 and the initial point $\left(\frac{k_s}{\mu_s}, 0, V_0, \frac{k_0}{\mu_0}, 0, 0, \frac{k_r}{\mu_r}, 0, \frac{k_{cr}}{\mu_{cr}}, 0\right)$, where $V_0 = 0.9 \times 10^{-3}$, indicates the amount of virus inoculated in a healthy person.

In Fig. 2a, we can see the viral dynamics when the proliferation parameter of cytotoxic cells (α_{ca}) is lower than proliferation parameter of activated B cells (α_a) and in the Fig. 2b we can see an increase (200 times) in the proliferation parameter α_a . In these cases, it is not possible to keep the viral load in low levels due to periodic oscillations. However, if there is an increase in the proliferation parameter of cytotoxic cells (100 times), it seems enough to avoid oscillations and to keep the viral load in low levels (see Fig. 2c). In this situation, the influence of the cytotoxic activity is fundamental to control the viral load. On the other hand, if there exists a weak cytotoxic response represented in a decrease in proliferation parameter α_{ca} but a strong humoral response represented in a increase of proliferation parameter α_a, we have two situations to avoid the oscillations. First, if the proliferation parameter α_{ca} is decreased ten fold and the proliferation parameter α_a is increased in one thousand fold, the oscillations disappear, and the infection is controlled (see Fig. 3a). Second, if there is an inhibition of Th0 cells differentiating into Th1 cells, i.e., $\gamma_2 \gg \gamma_1$, with γ_1 decreased in one hundred fold and the parameter α_a increased in ten fold, the viral load has a significant reduction(see Fig. 3b).

Previous results show that the cellular immune response affects more on the dynamics of the general model. Also, with a high proliferation of T_{ca} cells, it is possible to decrease the viral load to the level which laboratory tests can not detect the DENV in the body, although, mathematically, the viral load will always be nonzero. However, when the proliferation of B_a cells is not strong enough, the humoral immune response will not completely stop the infection by DENV, and it is necessary the usage of different strategies, like inhibition of differentiation of Th0 cells into Th1 cells.

5 Numerical simulation using parameters from literature and viral load data

Here we deal with global sensitivity analysis and parameter estimations.

5.1 Parameters from literature

The half life of monocytes/macrophages *in vivo* is between 1 and 2 months [5], so we assume the value $\mu_s = \frac{1}{60} = 0.017$ (dimensions of the parameters are given in Table 3, hence they are omitted in the text). The activated macrophages has a half life of 7 days and because the virus induces apoptosis [7,20], the death rate of the infected cells is taken as $\mu_I = 0.2$. There are on average 4×10^5 monocytes per milliliter of blood in humans [1], this will be the initial quantity of monocytes $S(0)$, so this implies that $k_s = \mu_s S(0) = 6.8 \times 10^3$. In healthy humans, the T-CD4+ and T-CD8+ cells survive on average 87 and 77 days, respectively [12], it means that the death rates μ_0, μ_1 and μ_2 have the same value 0.011, and $\mu_{cr} = 0.013$. The initial values of $T_0(0)$ and $T_{cr}(0)$ are 1×10^6 per milliliter of blood, which are the average quantities of T cells per milliliter of blood [1], thus $k_0 = \mu_0 T_0(0) = 1.1 \times 10^4$ and $k_{cr} = \mu_{cr} T_{cr}(0) = 1.3 \times 10^4$. The activated T-CD8+ cells have half life of a month approximately [28], then $\mu_{ca} = 0.03$. The B cells in rest have half life between 2 and

Table 2 Parameters of the humoral and cellular immune responses. Values assumed by some parameters are illustrative

Symbol	Definition	Value	Units
	Parameters of model		
k_s	Target cells production rate	0.034	$\text{ml}^{-1} \times \text{day}^{-1}$
k_0	Th helper cells production rate	0.011	$\text{ml}^{-1} \times \text{day}^{-1}$
β_I	Infection rate of target cells	0.87	$\text{ml} \times \text{day}^{-1}$
μ_s	Natural mortality rate of target cells	0.017	day^{-1}
μ_I	Apoptosis rate of infected cells	0.033	day^{-1}
μ_v	Decrease rate of dengue virus	2	day^{-1}
μ_0	Death rate of Th helper cells	0.011	day^{-1}
N_1	Virions released by infected cells on average	8	
N_2	Average of virions entrance into target cells	2	
k_{cr}	Naive cytotoxic cells production rate	0.011	$\text{ml}^{-1} \times \text{day}^{-1}$
α_I	Lysis rate of infected cells	0.8	$\text{ml} \times \text{day}^{-1}$
γ_1	Differentiation rate of Th helper cells into Th1 cells	0.01	$\text{ml} \times \text{day}^{-1}$
α_{cr}	Activation rate of naive cytotoxic cells into activated cytotoxic cells	0.8	$\text{ml} \times \text{day}^{-1}$
α_{ca}	Proliferation rate of activated cytotoxic cells	0.06	$\text{ml} \times \text{day}^{-1}$
μ_1	Death rate of Th1 helper cells	0.011	day^{-1}
μ_{cr}	Naive cytotoxic cells death rate	0.011	day^{-1}
μ_{ca}	Death rate of activated cytotoxic cells	0.033	day^{-1}
k_r	Naive B cells production rate	0.011	$\text{ml}^{-1} \times \text{day}^{-1}$
α_v	Phagocytocis rate of antigen-antibody complex	0.08	$\text{ml} \times \text{day}^{-1}$
γ_2	Differentiation rate of Th helper cells into Th2 cells	0.84	$\text{ml} \times \text{day}^{-1}$
α_r	Activation rate of naive B cells into activated B cells	0.7	$\text{ml} \times \text{day}^{-1}$
α_a	Proliferation rate of activated B cells	0.5	$\text{ml} \times \text{day}^{-1}$
μ_2	Death rate of Th2 helper cells	0.011	day^{-1}
μ_r	Naive B cells death rate	0.011	day^{-1}
μ_a	Death rate of activated B cells	0.033	day^{-1}

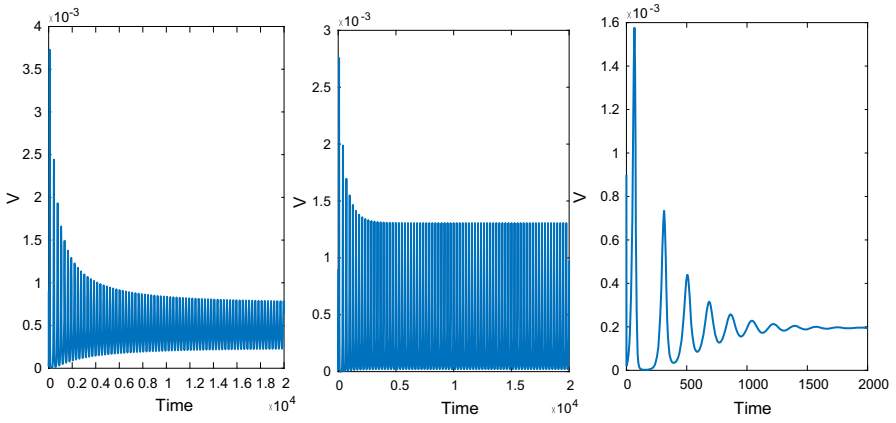

(a) $\alpha_{ca} = 0.06, \alpha_a = 0.5$ **(b)** $\alpha_{ca} = 0.06, \alpha_a = 100$ **(c)** $\alpha_{ca} = 6, \alpha_a = 0.5$

Fig. 2 The figure shows the viral dynamics when the proiliferation parameters of immune response are varied. **a** In this figure, we can see a weak immune response represented in a low proliferation of activated citotoxic cells and activated B cells. In this case, we have instability and the appearance of periodic oscillations. **b** In this figure, we see an increase of proliferation(α_a) of B_a cells and the parameter α_{ca} remains as before. This increase is not enough to prevent oscillations, that is, control or decrease of the viral load. **c** In this figure, we consider that the proliferation parameter of T_{ca} cells is increased in one hundred fold and the proliferation parameter of B_a cells remains as in (**a**). In this case, the viral load is decreased and there is no oscillations. This means that cytotoxic activity causes a strong influence on the decline of viral load

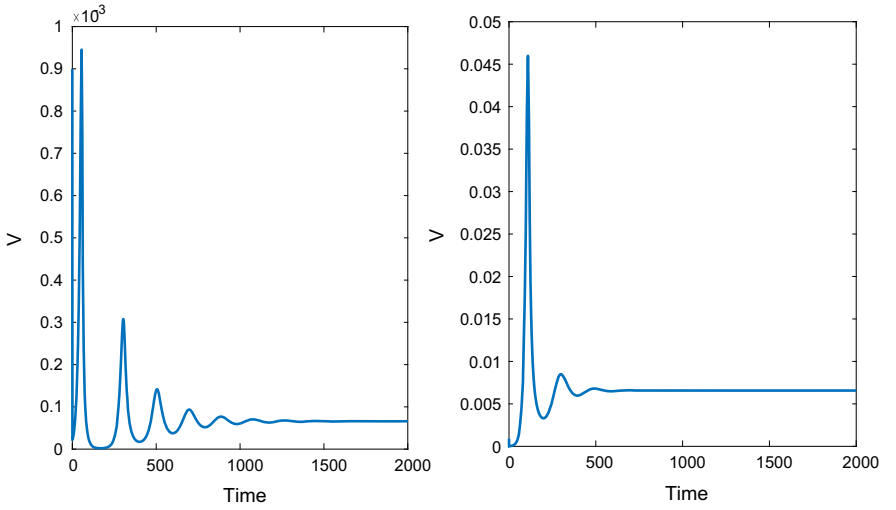

(a) $\alpha_{ca} = 0.006, \alpha_a = 500$ **(b)** $\alpha_{ca} = 0.006, \alpha_a = 5$, with $0.01 \times \gamma_1$

Fig. 3 The figure shows the viral dynamics and represents the way how the immune system acts with a weak cellular immune response to control the infection. **a** In this case, to avoid the oscillations, it is necessary a strong humoral immune represented in the proliferation of B_a cells. **b** This case describes the incapacity of the immune system to reduce the viral load only by the increasing the proliferation of B cells, for which it is necessary an inhibition of differentiation of T_0 cells into T_1 cells, implying in a reduction of parameter γ_1 with $\gamma_2 \gg \gamma_1$.

Table 3 Additional values for model parameters

Parameter	Definition	Value	Unit	Reference
k_s	Target cells production rate	6.8×10^3	$\text{ml}^{-1} \times \text{day}^{-1}$	[1,5]
k_0	Th helper cells production rate	1.1×10^4	$\text{ml}^{-1} \times \text{day}^{-1}$	[1,12]
k_r	Naive B cells production rate	5×10^5	$\text{ml}^{-1} \times \text{day}^{-1}$	[1]
k_{cr}	Naive citotoxic cells production rate	1.3×10^4	$\text{ml}^{-1} \times \text{day}^{-1}$	[1]
μ_s	Natural mortality rate of target cells	0.017	day^{-1}	[5]
μ_I	Apoptosis rate of infected cells	0.2	day^{-1}	[7,20]
μ_0	Death rate of Th helper cells	0.011	day^{-1}	[12]
μ_1	Death rate of Th1 helper cells	0.011	day^{-1}	[12]
μ_2	Death rate of Th2 helper cells	0.011	day^{-1}	[12]
μ_r	Naive B cells death rate	0.25	day^{-1}	[18]
μ_a	Death rate of activated B cells	0.02	day^{-1}	[18]
μ_{cr}	Naive cytotoxic cells death rate	0.013	day^{-1}	[12]
μ_{ca}	Death rate of activated cytotoxic cells	0.03	day^{-1}	[28]
N_1	Virions released by infected cells on average	5×10^4		[5,16]
N_2	Average of virions entrance into target cells	2		

4 days and more than 6 weeks if they are activated [18], which implies $\mu_r = 0.25$ and $\mu_a = 0.02$, respectively.

The quantity of B cells per milliliter of blood is around of 2×10^6 [1], thus $B(0) = 2 \times 10^6$, and as before we have $k_r = \mu_r B(0) = 5 \times 10^5$. The number of virions released by one infected cell is $N_1 = 5 \times 10^4$ [5,16], and we assume the value $N_2 = 2$.

A summary of these parameters and dimensions is presented in Table 3. The values of other parameters which are not presented in this table will be estimated in section 5.3.

5.2 Global uncertainty and sensitivity analysis

In mathematical models there are frequently many unknown parameters, therefore important questions that must be answered are concerned with the relationship of these parameters with the model outputs, in particular, which ones contribute most to output variability, and which ones require additional research or are insignificant. These questions can be answered using uncertainty and sensitivity analyses. We use the Latin hypercube sampling (Lhs) and Partial rank correlation coefficients (Prcc), and Extended Fourier amplitude sensitivity test (Efast) to assess global uncertainty and sensitivity analyses following the methodology proposed in [21]. The chosen days for these analyses were based on the viremia found in day two and day seven after infection because these times are crucial in the evolution of dengue infection: the onset of infection and the clearance. The parameters selected to perform global uncertainty and sensitivity analyses were β_I, α_v, γ_1, γ_2, α_r, α_{cr} and μ_v. We do not know the thresholds of these parameters except for the mortality rate of DENV μ_v.

Table 4 The Lhs with $N = 800$ and Prcc for the virus V in the days two and seven ($^{**}p$ value < 0.01)

Time	β_I	α_v	γ_2	α_r	α_I	γ_1
2	0.800394**	− 0.78303**	− 0.62821**	− 0.59711**		
7	− 0.63696**				− 0.35573**	− 0.42147**

Table 5 The Lhs with $N = 800$ and Prcc for the infected cells I in the days two and seven ($^{**}p$ value < 0.01)

Time	β_I	α_v	γ_2	α_r	α_I	γ_1
2	0.90099**	−065448**	−0.5645**	−0.55954**		
7	−0.6318**				−0.37803**	−0.42181**

The four serotypes of DENV have half life between 2.5 and 7.5 h [30]. The results of Lhs/Prcc for variable V show that in the day two, the effect of infection rate β_I is positively correlated (0.800394) with the viral load V. It means that if we increase this parameter, the viral load will rise, while the action of antibodies against virus α_v, the differentiation rate of T helper cells into Th2 cells, γ_2, and activation of the B cells, α_r, have negative correlations -0.78303, -0.62821, and -0.59711, respectively. The results of Lhs/Prcc for variable V in the day seven show an interesting fact: the infection rate β_I, the cytotoxic action rate α_I and the differentiation rate of T helper cells into Th1 γ_1 are negatively correlated (see Table 4).

The negative correlation of parameters α_I and γ_1 is due to the cytotoxic action rate α_I helping to decrease the infected cells and the differentiation rate γ_1 activates Th1 cells, which are crucial for the activation of cytotoxic activity. With respect to the negative correlation of parameter β_I, we can say that if we increase this infection rate, there are more infected cells helping Th0 cells to differentiate into Th1 cells that are capable of activating the cytotoxic activity of the T_{ca} cells. This suggests that cytotoxic activity is more important for the clearance of infection. Similar behaviors happen with the infected cells (see Table 5). The results of sensibility analysis by Efast are quite similar to those obtained by Lhs/Prcc. The parameters with high first order (S_i) and total order S_{T_i} sensitivity indexes are β_I, α_v and γ_2 in the second day, and in the seventh day, the parameters are α_I, γ_1 and α_{cr} (see Table 6). Similar results occur with the infected cells (data not shown).

5.3 Parameter estimation

In order to perform parameter estimations, we use real data from primary dengue fever of three patients with DENV1, DENV2, and DENV3, respectively. These data show the quantity of DENV in plasma (they can be accessed in the supplementary data in [6]). We used the parameters of Table 3 and genetic algorithm to find the best set of unknown parameters β_I, α_v, γ_1, γ_2, α_r, α_a, α_{cr}, α_{ca} and μ_v (see "Appendix A" for a short explanation). Table 7 shows the parameters estimated from data.

Table 6 The Efast with $Ns = 600$ for the virus V in the days two and seven ($^{*}p$value < 0.05 and $^{**}p$value < 0.01)

Time	β_I	α_v	γ_2	α_I	γ_1	α_{cr}
S_i						
2	0.0124**	0.0542**	0.0083*			
7	0.0135*	0.0143**	0.0126*	0.0135*	0.0265**	0.0131*
S_{T_i}						
2	0.6521**	0.8805**	0.6246*			
7	0.8706*	0.8751**	0.8589*	08731**	08694**	0.8538*

Table 7 Parameters estimated from three patients with dengue fever with serotypes 1, 2 and 3 (DENV-1, DENV-2 and DENV-3), respectively

Parameters	DENV-1	DENV-2	DENV-3	Units
β_I	5×10^{-8}	2.37×10^{-8}	5×10^{-8}	ml $\times$ day^{-1}
α_v	1.2×10^{-5}	2.34×10^{-5}	1.21×10^{-5}	ml $\times$ day^{-1}
γ_2	1.0×10^{-7}	2.48×10^{-5}	1.43×10^{-5}	ml $\times$ day^{-1}
α_r	1.6×10^{-7}	1.8×10^{-5}	1.61×10^{-5}	ml $\times$ day^{-1}
α_a	2.94×10^{-10}	2.1×10^{-12}	2.0×10^{-13}	ml $\times$ day^{-1}
α_I	1.6×10^{-5}	2.28×10^{-5}	1.41×10^{-5}	ml $\times$ day^{-1}
γ_1	1.13×10^{-4}	2.38×10^{-5}	1.3×10^{-5}	ml $\times$ day^{-1}
α_{cr}	1.21×10^{-7}	2.2×10^{-5}	1.41×10^{-5}	ml $\times$ day^{-1}
α_{ca}	4.89×10^{-7}	3.16×10^{-9}	4.0×10^{-11}	ml $\times$ day^{-1}
μ_v	3.3	3.5	3.3	day^{-1}

In all estimations we obtained high values for the proliferation parameter (α_{ca}) of activated T_{ca} cells in comparison with the proliferation parameter (α_a) of B_a cells, whereas the differentiation of Th0 cells into Th1 or Th2 cells is almost of the same order, which implies that the control of viral load and infected cells are obtained mostly by the cytotoxic activity but not exclusively. Indeed, we can see in the fittings of these parameters in Figs. 4, 5 and 6 that there is a little inhibition of activated T_{ca} cells and a strong response of B_a cells in the beginning of dengue infection. This could be a strategy of DENV to spread the virions because it will activate a greater amount of B cells, which will become into plasma cells that release antibodies with a not high affinity which may difficult the opsonization of pathogen. The clearance of the DENV happens when the antibodies improve its affinity and the cytotoxic cells respond to the right chemical signal. This allows the destruction of infected cells to prevent the release of new virus, which happens approximately on the fourth day (see Figs. 4, 5, 6).

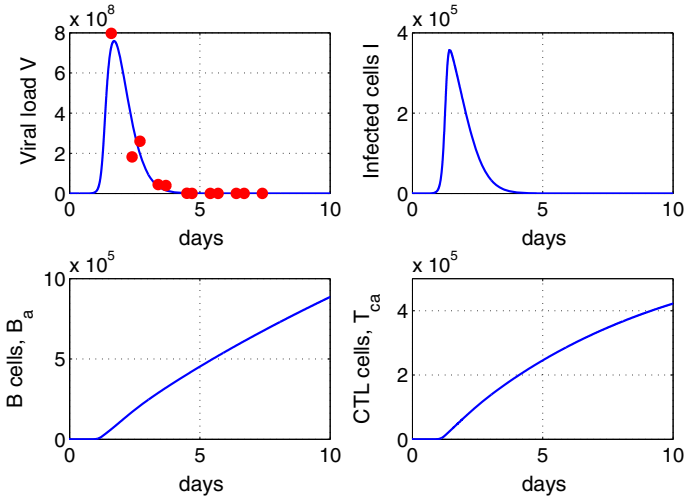

Fig. 4 The figure shows the virus, infected cells and immune response dynamics of primary dengue fever for a patient with virus serotype 1. The points indicated the viral load data. There exists a high response of B cells compared to T cells. (Color figure online)

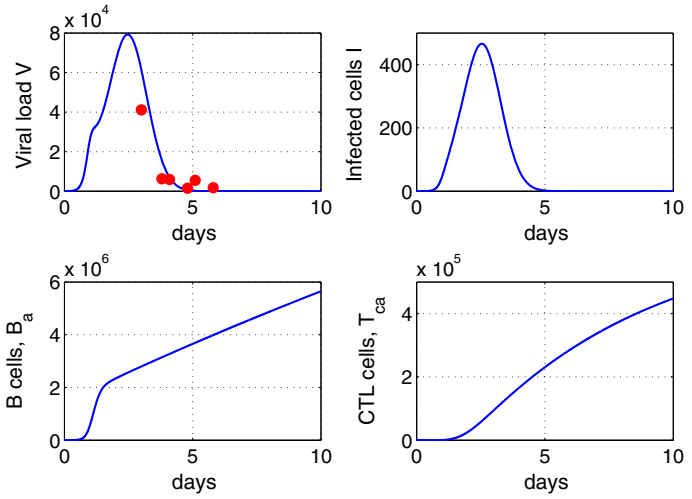

Fig. 5 The figure shows the virus, infected cells and immune response dynamics of primary dengue fever for a patient with virus serotype 2. The red points indicated the viral load data. There exists a high response of B cells compared to T cells. It is possible to observe that the response of T cells start after the B cells, showing a possible inhibition of this immune response. (Color figure online)

6 Discussion

In the present study, we developed a mathematical model of interaction between the immune system and dengue virus, which is a complex dynamics mediated by many factors. We proposed a model in which the cellular and humoral immune responses

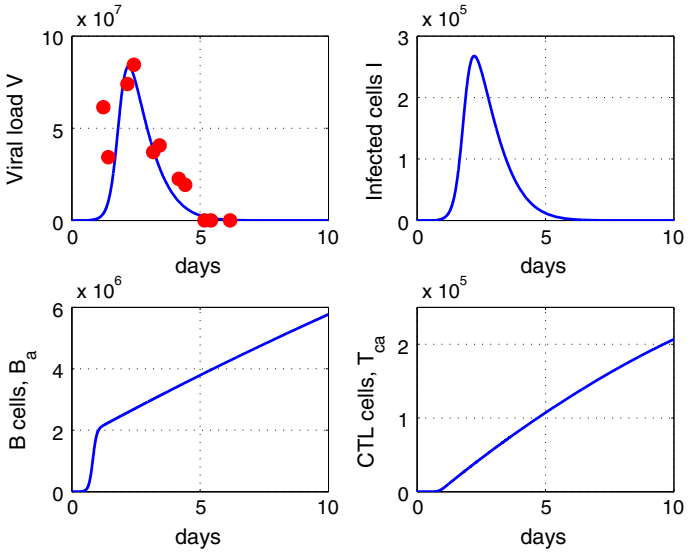

Fig. 6 The figure shows the virus, infected cells and immune response dynamics of primary dengue fever for a patient with virus serotype 3. The points indicated the viral load data. There exists a high response of B cells compared to T cells and the cellular immune response is inhibited initially but strongly activated in the end. (Color figure online)

depend on the differentiation of Th0 helper cells into Th1 and Th2 cells. We showed that the virus-free equilibrium is globally asymptotically stable if the basic reproduction number is less than one, which could be interpreted like the effectively answer of innate immune response to stop the dengue virus infection. Finally, the stability analysis of virus presence equilibrium showed that the dynamics of the general model is mostly affected by the cellular immune response. A strong cellular immune response will be enough to control the viral load and avoid oscillations. Meanwhile, a weak response in the proliferation of cytotoxic cells will generate oscillations and the appearance of a limit cycle. There exist two ways to change this behavior. The first is a strong proliferation of activated B cells, which will generate an improvement in the fitness of antibodies to stop the infection. The second is inhibition of the differentiation of Th0 cells into Th1 cells, which means that activation of cytotoxic cells should be low. In this way, the immune response would predominantly be the humoral immune response, and the dynamical system will has no oscillations.

By using the parameters from the medical literature and performing fittings of unknown parameters of the model through the use of clinical data on dengue fever, we showed that there is more proliferation of cytotoxic cells than B cells. This is evident in the values of the proliferation parameter of activated cytotoxic cells, α_{ca}, which are higher than the values of the proliferation parameter of activated B cells, α_a. These values assure the control of infection, avoid oscillations and suggest a dominant cellular immune response in relation to the humoral immune response.

Finally, the simulations showed that the initial humoral immune response is faster than the cellular immune response at the onset of infection, but the cellular immune response acts strongly in clearance. This means that the cellular immune response is inhibited in the beginning of infection as a possible strategy used by the virus to spread through the body, because the large number of activated B cells will release initially low affinity antibodies which may difficult the opsonization of pathogen and it may be a clue to answer why the antibodies can help in the enhancement of second infections. In fact, in vitro studies of dengue infections in dendritic cells reported a notably suppressed proliferation of T cells [26,31], and some studies with patients showed an increase T-CD8+ cell counts later in the course of disease [8,23]. Other models considering the role of cytokines have to be considered to better analyze the role of the T-CD8+ cells in the control of the viral replication and the balance between humoral and cellular immune responses.

Acknowledgements This study was supported by research Grant 2013/17264-0, São Paulo Research Foundation (FAPESP)

Appendices

A Genetic Algorithm

The function to be minimized is $f(V, \Upsilon) = (V - V_{data})^2$, where V is the viral load, given by positive solution of the system (1)–(4) at steady state, V_{data} are the data of viral load of patients and $\Upsilon = (\beta_I, \alpha_v, \gamma_1, \gamma_2, \alpha_r, \alpha_a, \alpha_{cr}, \alpha_{ca}, \mu_v)$ is the set of the unknown parameters, where $\beta_I \in (\beta_{Imin}, \beta_{Imax})$, $\alpha_v \in (\alpha_{vmin}, \alpha_{vmax})$, ..., $\mu_v \in (\mu_{vmin}, \mu_{vmax})$. The first step is the transformation of each parameter in binary and form a string called chromosome. Let Γ be the binary representation of Υ. Then

$$\Gamma = (\beta_{I2}\alpha_{v2}\gamma_{12}\gamma_{22}\alpha_{r2}\alpha_{a2}\alpha_{cr2}\alpha_{ca2}\mu_{v2})$$

will be the chromosome, which has just 1's and 0's and $\beta_{I2}, \alpha_{v2}, \gamma_{12}, \gamma_{22}, \alpha_{r2}, \alpha_{a2}, \alpha_{cr2}$, α_{ca2} and μ_{v2} are the binary representation of parameters. This chromosome has length $m = \sum_{i=1}^{9} m_i$, where m_1 is the smallest integer such that $(\beta_{Imax} - \beta_{Imin}) \times 10^p < 2^{m_1} - 1$, m_2 is the smallest integer such that $(\alpha_{vmax} - \alpha_{vmin}) \times 10^p < 2^{m_2} - 1, \ldots,$ m_9 is the smallest integer such that $(\mu_{vmax} - \mu_{vmin}) \times 10^p < 2^{m_9} - 1$ and p is the number indicating decimal places desirable for the parameters. Each m_i is the length of binary string of parameters.
The algorithm is:

1. **Initial population**
   We create a random population P_0 of chromosomes, where each chromosome is a binary string of length $m = \sum_{i=1}^{9} m_i$. We suppose that this initial population has n chromosomes, i.e.,
   $$P_0 = \{\Gamma_0^1, \ldots, \Gamma_0^n\}.$$

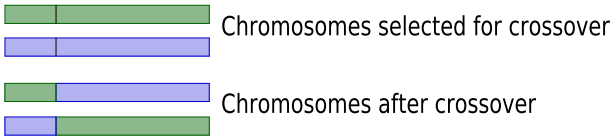

Fig. 7 The one-point crossover in two chromosome

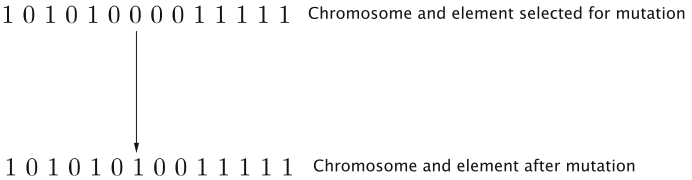

Fig. 8 The mutation operator

2. **Evaluation of function**
   At this step we evaluate the function f at each element of the population P_0, that is, $f(V, \Upsilon^i)$, where Υ^i is the decimal representation of Γ_0^i, $i = 1, \ldots, n$.
3. **Next Population**
   At this step we select the next population by applying the genetic operator (crossover and mutations).

   - **Selection method**
     In order to select the population, we apply the tournament selection method, which consists in selecting randomly some number k of chromosome and storing the minimum of the set $\{f(V, \Upsilon^{J_1}), \ldots, f(V, \Upsilon^{J_k})\}$ of k elements, where J is a subset of k elements ($J \subset \{1, 2, \ldots, n\}$), into the next generation. This process is repeated n times. Obviously, some chromosomes would be selected more than once. Now, we apply the crossover and mutations operators to this selected population.

   - **Crossover operator**
     This operator apply recombination in the chromosomes (see Fig. 7). We give the probability of crossover p_c. This probability gives us the expected number $p_c \times n$ of chromosomes, which undergo the crossover operation. The process of crossover function is done in the following way: for each chromosome in the (new) population, we generate a random number r from the range [0, 1]. If $r < p_c$, we select this chromosome for crossover.
     If the number of selected chromosomes is even, we can pair them easily. If the number of selected chromosomes were odd, we would either add one extra chromosome or remove one selected chromosome, which is made randomly as well. The operator explained here is known as one-point crossover. There are other crossover operator as: two-point crossover, uniform crossover and half uniform crossover.

   - **Mutation operator**
     This operator applies alterations in the elements of chromosomes (changes of 0 for 1 and vice versa (see Fig. 8). We give the probability of mutation p_m. This

probability gives us the expected number of mutated elements $p_m \times m \times_n$. The process to perform the mutation operator is similar to the crossover operator: for each chromosome in the current (i.e., after crossover) population and for each element within the chromosome, a random number r is generated in the range [0, 1]. If $r < p_m$, then we mutate the element.

4. After all the above steps, we have created the first generation: population P_1. Now just repeat the steps 2 and 3 to P_1, and the process goes up to the desired generations.

A detailed explanation of genetic algorithms can be found in [22]. The algorithm adapted and used in the simulations can be accessed in the link http://people.csail.mit.edu/gbezerra/Code/GA/ga.m.

References

1. Alberts, B., et al.: Molecular Biology of the Cell, 4th edn. Garland Science, New York (2002)
2. Ansari, H., Hesaaraki, M.: A with-in host dengue infection model with immune response and beddington-deangelis incidence rate. Appl. Math. **3**(02), 177 (2012)
3. Ben-Shachar, R., Koelle, K.: Minimal within-host dengue models highlight the specific roles of the immune response in primary and secondary dengue infections. J. R. Soc. Interface **12**(103), 20140886 (2015)
4. Cerón Gómez, M., Yang, H.M.: A simple mathematical model to describe antibody-dependent enhancement in heterologous secondary infection in dengue. Math. Med. Biol. J. IMA **36**, 411–438 (2019)
5. Chen, Y.-C., Wang, S.-Y.: Activation of terminally differentiated human monocytes/macrophages by dengue virus: productive infection, hierarchical production of innate cytokines and chemokines, and the synergistic effect of lipopolysaccharide. J. Virol. **76**(19), 9877–9887 (2002)
6. Clapham, H.E., et al.: Within-host viral dynamics of dengue serotype 1 infection. J. R. Soc. Interface **11**(96), 20140094 (2014)
7. Courageot, M.-P., Catteau, A., Despres, P.: Mechanisms of dengue virus-induced cell death. Adv. Virus Res. **60**, 157–186 (2003)
8. de Matos, A.M., et al.: CD8+ T lymphocyte expansion, proliferation and activation in dengue fever. PLoS Negl. Trop. Diseases **9**(2), e0003520–e0003520 (2015)
9. Esteva, L., Yang, H.M.: Assessing the effects of temperature and dengue virus load on dengue transmission. J. Biol. Syst. **23**(4), 527–554 (2015)
10. Gantmacher, F.R., Brenner, J.L.: Applications of the Theory of Matrices. Dover Publications, New York (2005)
11. Gujarati, T.P., Ambika, G.: Virus antibody dynamics in primary and secondary dengue infections. J. Math. Biol. **69**(6–7), 1773–1800 (2014)
12. Hellerstein, M., et al.: Directly measured kinetics of circulating T lymphocytes in normal and HIV-1-infected humans. Nat. Med. **5**(1), 83–89 (1999)
13. Hwang, T.-W., Wang, F.-B.: Dynamics of a dengue fever transmission model with crowding effect in human population and spatial variation. Discrete Contin. Dyn. Syst. Ser. B **18**(1), 147–161 (2013)
14. Karl, S., Halder, N., Kelso, J.K., Ritchie, S.A., Milne, G.J.: A spatial simulation model for dengue virus infection in urban areas. BMC Infectious Dis. **14**(1), 447 (2014)
15. Knipe, D.M., Howley, P.M., Griffin, D., Lamb, R., Martin, M., Roizman, B., Straus, S.: Fields Virology. Lippincott Williams & Wilkins, Philadelphia (2001)
16. Kou, Z., et al.: Human antibodies against dengue enhance dengue viral infectivity without suppressing type i interferon secretion in primary human monocytes. Virology **410**(1), 240–247 (2011)
17. Macdonald, G.: The analysis of equilibrium in malaria. Trop. Dis. Bull. **49**(9), 813–829 (1952)
18. Mak, T.W., Saunders, M.E.: The Immune Response: Basic and Clinical Principles. Academic Press, Berlin (2005)
19. Mandell, G., Bennett, J.E., Dolin, R.: Principles and Practices of Infectious Diseases, 7th edn. Churchill Livingstone Elsevier, Philadelphia (2010)

20. Marianneau, P., Flamand, M., Deubel, V., Desprès, P.: Induction of programmed cell death (apoptosis) by dengue virus in vitro and in vivo. Acta Cient. Venez. **49**, 13–17 (1997)
21. Marino, S., et al.: A methodology for performing global uncertainty and sensitivity analysis in systems biology. J. Theor. Biol. **254**(1), 178–196 (2008)
22. Michalewicz, Z.: Genetic Algorithms + Data Structures= Evolution Programs, 3rd edn. Springer, Berlin (1996)
23. Myint, K.S., et al.: Cellular immune activation in children with acute dengue virus infections is modulated by apoptosis. J. Infect. Dis. **194**(5), 600–607 (2006)
24. Nikin-Beers, R., Ciupe, S.M.: The role of antibody in enhancing dengue virus infection. Math. Biosci. **263**, 83–92 (2015)
25. Nuraini, N., et al.: A with-in host dengue infection model with immune response. Math. Comput. Model. **49**(5), 1148–1155 (2009)
26. Palmer, D.R., et al.: Differential effects of dengue virus on infected and bystander dendritic cells. J. Virol. **79**(4), 2432–2439 (2005)
27. Perera, S., Perera, S.: Simulation model for dynamics of dengue with innate and humoral immune responses. In: Computational and Mathematical Methods in Medicine (2018)
28. Ribeiro, R.M., et al.: In vivo dynamics of T cell activation, proliferation, and death in HIV-1 infection: Why are CD4+ but not CD8+ T cells depleted? Proc. Natl. Acad. Sci. **99**(24), 15572–15577 (2002)
29. Sasmal, S.K., Dong, Y., Takeuchi, Y.: Mathematical modeling on t-cell mediated adaptive immunity in primary dengue infections. J. Theor. Biol. **429**, 229–240 (2017)
30. Sithisarn, P., et al.: Behavior of the dengue virus in solution. J. Med. Virol. **71**(4), 532–539 (2003)
31. Sun, P., et al.: CD40 ligand enhances dengue viral infection of dendritic cells: a possible mechanism for T cell-mediated immunopathology. J. Immunol. **177**(9), 6497–6503 (2006)
32. Yang, H.M.: The basic reproduction number obtained from jacobian and next generation matrices-a case study of dengue transmission modelling. Biosystems **126**, 52–75 (2014)
33. Yang, H.M.: A mathematical model to assess the immune response against trypanosoma cruzi infection. J. Biol. Syst. **23**(01), 131–163 (2015)
34. Yang, H.M.: The transovarial transmission in the dynamics of dengue infection: epidemiological implications and thresholds. Math. Biosci. **286**, 1–15 (2017)
35. Yang, H.M., Boldrini, J.L., Fassoni, A.C., Freitas, L.F.S., Gomez, M.C., de Lima, K.K.B., Andrade, V.R., Freitas, A.R.R.: Fitting the incidence data from the city of Campinas, Brazil, based on dengue transmission modellings considering time-dependent entomological parameters. PLoS ONE **11**(3), e0152186 (2016)
36. Yang, H.M., Macoris, M.L.G., Galvani, K.C., Andrighetti, M.T.M., Wanderley, D.M.V.: Assessing the effects of temperature on dengue transmission. Epidemiol. Infect. **137**(08), 1179–1187 (2009)

Publisher's Note Springer Nature remains neutral with regard to jurisdictional claims in published maps and institutional affiliations.